STUDY ON A MAGNETIC LEVITATION FLYWHEEL ENERGY STORAGE DEVICE

Jianrong Cao
TLBI, Xi' an Jiaotong University, Xi' an, China, caojianrong@tlbi.xjtu.edu.cn
Lie Yu
TLBI, Xi' an Jiaotong University, Xi' an, China
Youbai Xie
TLBI, Xi' an Jiaotong University, Xi' an, China

ABSTRACT
A kind of flywheel energy storage device based on magnetic levitation has been studied. A decoupling control approach has been developed for the nonlinear model of the flywheel energy storage device supported by active magnetic bearings such that the unstability brought by gyroscopic effects can be overcome. A NdFeB high field permanent-magnet synchronous motor/generator has been employed as the apparatus of the energy transform, with which power is provided from and to flywheel. To verify the performance of the system, some simulations are employed, and results are satisfactory. A prototype was made to experiment.

INTRODUCTION
There are many kinds of energy, such as heat energy, light energy, electric energy and mechanical energy. Some kinds of energy can be stored into various batteries. Flywheel battery is a kind of energy storage devices in which rotor kinetic energy is stored while it rotates. It is known that the kinetic energy of a rotor system is proportional to moment of inertia around its rotational axis, and to square of its rotational speed. When a flywheel rotor system is accelerated to an ultra-high speed, the kinetic energy is able to be in the extreme large. So electric energy can be provided to the flywheel as it is accelerated, whereas the flywheel can deliver electric energy. In a flywheel system, a motor/generator can be employed to provide power to and from the flywheel. To minimize losses during the system standby, power loading or unloading, active magnetic bearings are supposed to use due to their contact free operation. Furthermore, vacuum housing is able to reduce the friction losses. However, because of larger moment of inertia around rotational axis compared with around radial axis, strongly rotor gyroscopic effects may make the rotor unstable. To avoid it, the influence of gyroscopic effects has to be considered. The main goal of this paper is the study of the decoupling control as well as input-output linearization for the flywheel energy storage system in which the rotor is supported by active magnetic bearings so that the problem brought by rotor gyroscopic effects is overcome.

In this paper, a kind of flywheel energy storage device based on magnetic levitation has been studied. The system includes two active radial magnetic bearings and a passive permanent-magnet thrust bearing. A decoupling control approach has been developed for the nonlinear model of the flywheel rotor supported by active magnetic bearings. A nonlinear controller based on dynamic feedback linearization is designed such that the strongly coupled rotor motion is reduced to five normalization linear subsystems including four rotor radial displacements and the rotor speed. These linear subsystems are completely decoupled, so they are not influencing each other. The linearized system improves the transient response of the system. For these linearized subsystems, linear controllers are created. A high field permanent-magnet synchronous motor/generator has been employed as the apparatus of the energy transform, with which the rotor speed of 40,000 rpm has been gained and about 0.5kWh energy is provided from and to flywheel. Some simulations are employed to verify the performance of the system, and results are satisfactory. A prototype was made to experiment.

PRINCIPLE OF THE FLYWHEEL BATTERY[1]
Fig.1 shows the configuration of the flywheel energy storage device. The system employed two radial active magnetic bearings and a passive thrust magnetic bearing (PMB). A high field NdFeB permanent-magnet synchronous motor /generator (PMSM) is used as the apparatus of the energy transform, with which power is provided from and to flywheel. The AMBs make the rotor levitate, and the PMB carries the weight of the

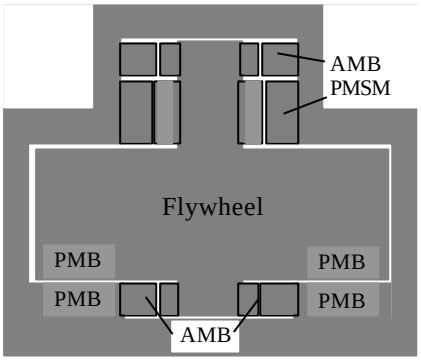

FIGURE 1: Configuration of the Flywheel Battery

flywheel. When the battery is charged, electric energy can be provided to the flywheel while it is accelerated, whereas the flywheel can deliver electric energy.

MODELING

The dynamics of the rotor-magnetic bearing system will be described in this section. A rotor model of two current biased radial active magnetic bearings is represented in Fig.2, where B_1, B_2 denote upper and lower AMB, respectively. The relationship between the magnetic force $\boldsymbol{F}$ acting on the rotor, and the coil current $\boldsymbol{i}$ as well as rotor's displacement $\boldsymbol{e}$ can be written as

$$\boldsymbol{F} = k_e\,\boldsymbol{e} + k_i\,\boldsymbol{i} \tag{1}$$

where $\boldsymbol{F} = (F_{x1}, F_{x2}, F_{y1}, F_{y2})^T$, $\boldsymbol{e} = (x_1, x_2, y_1, y_2)^T$, and $\boldsymbol{i} = (i_{x1}, i_{x2}, i_{y1}, i_{y2})^T$.

Thus

$$\begin{cases} \boldsymbol{F}_{x1} = k_e x_1 + k_i i_{x1} \\ \boldsymbol{F}_{x2} = k_e x_2 + k_i i_{x2} \\ \boldsymbol{F}_{y1} = k_e y_1 + k_i i_{y1} \\ \boldsymbol{F}_{y2} = k_e y_2 + k_i i_{y2} \end{cases} \tag{2}$$

where (x_1, y_1, x_2, y_2) is the bearing coordinate system. The first term of the right-hand side of (1) describes the displacement stiffness; the second term describes the current stiffness. In equation (2), k_e is stiffness coefficient of displacement, and k_i is that of current for the AMBs. The subscript x and y means being in x and y directions, and 1 and 2 denote B1 and B2, respectively. To gain an exact model of the system, Finite Element Method (FEM) is employed to calculate these coefficients.

Assuming that the rotor is rigid, we can write the equations of motion in the mass center coordinate $(x_g, y_g, z_g, \boldsymbol{j}, \boldsymbol{y})$ as [2]

$$\begin{cases} m\,\ddot{x}_g + \boldsymbol{F}_{x1} + \boldsymbol{F}_{x2} = f_x \\ m\,\ddot{y}_g + \boldsymbol{F}_{y1} + \boldsymbol{F}_{y2} = f_y \\ I\dot{\boldsymbol{j}} - \boldsymbol{w}_r J\dot{\boldsymbol{y}} = l_1\boldsymbol{F}_{x1} - l_2\boldsymbol{F}_{x2} \\ I\dot{\boldsymbol{y}} + \boldsymbol{w}_r J\dot{\boldsymbol{j}} = l_1\boldsymbol{F}_{y1} - l_2\boldsymbol{F}_{y2} \\ J\dot{\boldsymbol{w}}_r = \boldsymbol{T}_e \\ \boldsymbol{F}_z = mg + m\ddot{z}_g \end{cases} \tag{3}$$

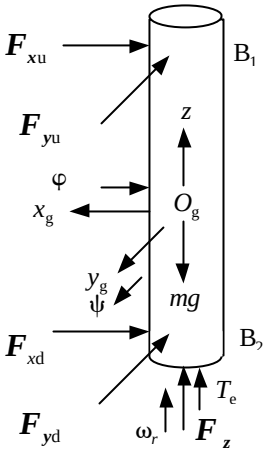

FIGURE 2: Rotor Model

where $\boldsymbol{w}_r$ is the rotor speed, f_x and f_y are disturbances created by the unbalance of the rotor, J and I are moments of inertia around rotation and radial axis, respectively, T_e is torque of the motor, and l_1, l_2 are the distances of the upper and lower magnetic bearings. As the control is performed in the bearing coordinate (x_1, x_2, y_1, y_2), we have to do coordinate transformation, i.e.

$$\begin{cases} x_1 = x_g - l_1\boldsymbol{j} \\ x_2 = x_g + l_2\boldsymbol{j} \\ y_1 = y_g - l_1\boldsymbol{y} \\ y_2 = y_g + l_2\boldsymbol{y} \end{cases} \tag{4}$$

From (2)-(4), we can obtain the state representation as follows

$$\begin{cases} \dot{\boldsymbol{x}}_1 = \boldsymbol{x}_3 \\ \dot{\boldsymbol{x}}_2 = \boldsymbol{x}_4 \\ \dot{\boldsymbol{x}}_3 = -\dfrac{1}{m}\left(2k_e\boldsymbol{x}_1 + k_e(l_2 - l_1)\boldsymbol{x}_5 + k_i u_1 + k_i u_2\right) + \dfrac{f_x}{m} \\ \dot{\boldsymbol{x}}_4 = -\dfrac{1}{m}\left(2k_e\boldsymbol{x}_2 + k_e(l_2 - l_1)\boldsymbol{x}_6 + k_i u_3 + k_i u_4\right) + \dfrac{f_y}{m} \\ \dot{\boldsymbol{x}}_5 = \boldsymbol{x}_7 \\ \dot{\boldsymbol{x}}_6 = \boldsymbol{x}_8 \\ \dot{\boldsymbol{x}}_7 = \dfrac{J}{I}\boldsymbol{x}_9\boldsymbol{x}_8 - \dfrac{k_e(l_2 - l_1)}{I}\boldsymbol{x}_1 - \dfrac{k_e\left(l_1^2 + l_2^2\right)}{I}\boldsymbol{x}_5 \\ \qquad + \dfrac{k_i l_1}{I}u_1 - \dfrac{k_i l_2}{I}u_2 \\ \dot{\boldsymbol{x}}_8 = \dfrac{J}{I}\boldsymbol{x}_9\boldsymbol{x}_7 - \dfrac{k_e(l_2 - l_1)}{I}\boldsymbol{x}_1 - \dfrac{k_e\left(l_1^2 + l_2^2\right)}{I}\boldsymbol{x}_6 \\ \qquad + \dfrac{k_i l_1}{I}u_1 - \dfrac{k_i l_2}{I}u_2 \\ \dot{\boldsymbol{x}}_9 = \dfrac{1}{J}u_5 \end{cases} \tag{5}$$

where we defined $x = (x_1, x_2, x_3, x_4, x_5, x_6, x_7, x_8, x_9)^T = (x_g, y_g, \dot{x}_g, \dot{y}_g, \boldsymbol{j}, \boldsymbol{y}, \dot{\boldsymbol{j}}, \dot{\boldsymbol{y}}, \boldsymbol{w}_r)^T$ is the state variable, $\boldsymbol{U} = (u_1, u_2, u_3, u_4, u_5)^T = (i_{x1}, i_{x2}, i_{y1}, i_{y2}, T_e)^T$ is input variable.

DECOUPLING CONTROL

Let the outputs be the displacements of the rotor and its speed, i.e.,

$$Y = \begin{pmatrix} x_1 \\ x_2 \\ y_1 \\ y_2 \\ \boldsymbol{w}_r \end{pmatrix} = \begin{pmatrix} \boldsymbol{x}_1 - l_1\boldsymbol{x}_5 \\ \boldsymbol{x}_1 + l_2\boldsymbol{x}_5 \\ \boldsymbol{x}_2 - l_1\boldsymbol{x}_6 \\ \boldsymbol{x}_2 + l_2\boldsymbol{x}_6 \\ \boldsymbol{x}_9 \end{pmatrix} \tag{6}$$

for the control variables u_1 - u_5 to appear in the output equation, it is necessary to differentiate $\boldsymbol{Y}$, which gives equation (7).

$$\begin{pmatrix} \ddot{y}_1 \\ \ddot{y}_2 \\ \ddot{y}_3 \\ \ddot{y}_4 \\ \dot{y}_5 \end{pmatrix} = \begin{pmatrix} \ddot{\boldsymbol{x}}_1 - l_u\ddot{\boldsymbol{x}}_5 \\ \ddot{\boldsymbol{x}}_1 + l_d\ddot{\boldsymbol{x}}_5 \\ \ddot{\boldsymbol{x}}_2 - l_u\ddot{\boldsymbol{x}}_6 \\ \ddot{\boldsymbol{x}}_2 + l_d\ddot{\boldsymbol{x}}_6 \\ \dot{\boldsymbol{x}}_9 \end{pmatrix} = \begin{pmatrix} \dot{\boldsymbol{x}}_3 - l_u\dot{\boldsymbol{x}}_7 \\ \dot{\boldsymbol{x}}_3 + l_d\dot{\boldsymbol{x}}_7 \\ \dot{\boldsymbol{x}}_4 - l_u\dot{\boldsymbol{x}}_8 \\ \dot{\boldsymbol{x}}_4 + l_d\dot{\boldsymbol{x}}_8 \\ \dot{\boldsymbol{x}}_9 \end{pmatrix} \tag{7}$$

Sign

$$\begin{cases} k_{iu} = -k_i\left(1 + \dfrac{ml_u^2}{I}\right) \\ k_{id} = -k_i\left(1 + \dfrac{ml_d^2}{I}\right) \\ k_{iud} = -k_i\left(1 - \dfrac{ml_u l_d}{I}\right) \end{cases} \tag{8}$$

and

$$\begin{cases} k_1 = k_e\left(-\dfrac{2}{m} + \dfrac{l_u(l_d - l_u)}{I}\right) \\ k_2 = k_e\left(-\dfrac{2}{m} - \dfrac{l_d(l_d - l_u)}{I}\right) \\ k_3 = k_e\left(-\dfrac{l_d - l_u}{m} + \dfrac{l_u(l_u^2 + l_d^2)}{I}\right) \\ k_4 = k_e\left(-\dfrac{l_d - l_u}{m} - \dfrac{l_d(l_u^2 + l_d^2)}{I}\right) \end{cases} \tag{9}$$

Let

$$\begin{cases} \boldsymbol{j}_1 = m\ddot{x}_{1ref} \\ \boldsymbol{j}_2 = m\ddot{x}_{2ref} \\ \boldsymbol{j}_3 = m\ddot{y}_{1ref} \\ \boldsymbol{j}_4 = m\ddot{y}_{2ref} \\ \boldsymbol{j}_5 = J\dot{\boldsymbol{w}}_{rref} \end{cases} \tag{10}$$

where the variables with subscript *ref* denote desired ones.

Furthermore, let

$$\begin{cases} v_1 = \boldsymbol{j}_1 - k_1m\boldsymbol{x}_1 - k_3m\boldsymbol{x}_5 + \dfrac{ml_uJ}{2I}\boldsymbol{x}_9\boldsymbol{x}_8 \\ v_2 = \boldsymbol{j}_2 - k_2m\boldsymbol{x}_1 - k_4m\boldsymbol{x}_5 - \dfrac{ml_dJ}{2I}\boldsymbol{x}_9\boldsymbol{x}_8 \\ v_3 = \boldsymbol{j}_3 - k_1m\boldsymbol{x}_2 - k_3m\boldsymbol{x}_6 + \dfrac{ml_uJ}{2I}\boldsymbol{x}_9\boldsymbol{x}_7 \\ v_4 = \boldsymbol{j}_4 - k_2m\boldsymbol{x}_2 - k_4m\boldsymbol{x}_6 - \dfrac{ml_dJ}{2I}\boldsymbol{x}_9\boldsymbol{x}_7 \\ v_5 = \boldsymbol{j}_5 \end{cases} \tag{11}$$

To linearize the system using dynamic feedback, the input currents for AMBs and the torque for the PMSM are set as

$$\begin{cases} u_1 = \dfrac{1}{k_{iu}k_{id} - k_{iud}^2}\left(k_{id}v_1 - k_{iud}v_2\right) \\ u_2 = \dfrac{1}{k_{iu}k_{id} - k_{iud}^2}\left(k_{iu}v_2 - k_{iud}v_1\right) \\ u_3 = \dfrac{1}{k_{iu}k_{id} - k_{iud}^2}\left(k_{id}v_3 - k_{iud}v_4\right) \\ u_4 = \dfrac{1}{k_{iu}k_{id} - k_{iud}^2}\left(k_{iu}v_4 - k_{iud}v_3\right) \\ u_5 = v_5 \end{cases} \tag{12}$$

After substituting (12) in (5), (7), we can obtain the normalization linear system (13). The nonlinear magnetic bearing system thus is transformed into five linear decoupled subsystems without internal dynamics.

$$\begin{cases} \ddot{x}_1 = \dfrac{1}{m}j_1 \\ \ddot{x}_2 = \dfrac{1}{m}j_2 \\ \ddot{y}_1 = \dfrac{1}{m}j_3 \\ \ddot{y}_2 = \dfrac{1}{m}j_4 \\ \dot{w}_r = \dfrac{1}{J}j_5 \end{cases} \tag{13}$$

where $\boldsymbol{F} = (\boldsymbol{j}_1, \boldsymbol{j}_2, \boldsymbol{j}_3, \boldsymbol{j}_4, \boldsymbol{j}_5)^T$ is new input vector for decoupled linearization system. Decoupling control scheme can be shown in Fig.3.

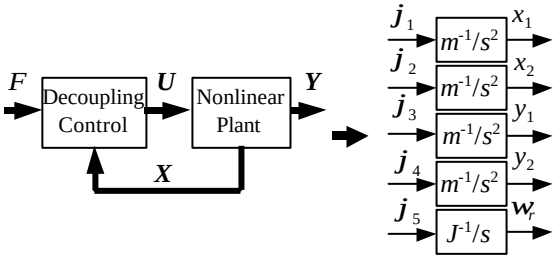

FIGURE 3: Decoupling Control via Feedback Linearization

From equation (13) we can know that these subsystems, including four radial displacements of the rotor and its speed, are multiple-integrator form. Thus, after using feedback linearization control, linear control system techniques can be applied to these linear subsystems to synthesize desired response.

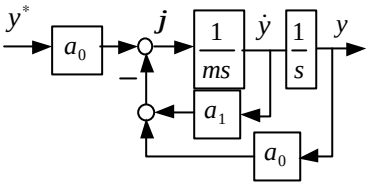

FIGURE 4: Closed-loop control of displacement

Next, the regulation of displacements of the rotor to desired values is ensured via utilizing state-variable feedback. A simple illustration of the state-variable feedback method is depicted in Fig.4. Each of closed-loop transfer functions of displacement's subsystems becomes

$$\frac{y(s)}{i(s)} = \frac{a_0 / m}{s^2 + a_1 / m \cdot s + a_0 / m} \qquad (14)$$

where y represents each displacement of AMBs, and i does control current, respectively. They are all typical second-order linear systems. The parameter a_0 depends on bandwidth of the system, supply voltage of the power amplifier, and so on. The parameter a_1 decides damping factor of the system. In addition, the rotor speed can be regulated via PI controller, which had been published in our another paper [8].

AXIAL STABILITY

A passive thrust magnetic bearing system has designed, in which high field permanent magnets are employed. The magnets have the shape of a ring and are magnetized in thrust direction. One ring is mounted on the flywheel rotor; the other is attached to the stator (see Fig.5). Its stiffness is about 4.25×10^4 N / m.

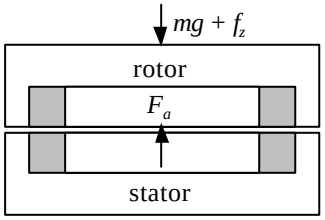

FIGURE 5: Passive Axial Magnetic Bearing

We have also studied active axial magnetic bearing without premagnetization in a turbo molecular pump [7], it can arrive at higher stiffness.

SIMULATION AND EXPERIMENT RESULTS

To verify the effectiveness of the proposed scheme, some simulations are employed with simulation tool SIMULINK in the mathematics software package MATLAB. A prototype was made to experiment. The PMSM in the flywheel energy storage device can arrive at higher speed than 40,000 rpm.

Simulation

Here, we consider simulating the proposed decoupling control scheme. Table 1 shows the mainly parameters of the system.

TABLE 1: Data of the Flywheel System

mass of the rotor: m	7.25 kg
axial inertia momentum: J	0.21 kg m^2
radial inertia momentum: I	0.032 kg m^2
nominal air-gap: e	0.4 mm
factor of unbalance of rotor: e_0	1×10^{-6} m
power of the motor	4.2 kW
nominal speed	40,000 rpm

Fig.6 shows simulation result of step response of rotor displacements. It can be seen that the percent overshoot is less than 5 %.

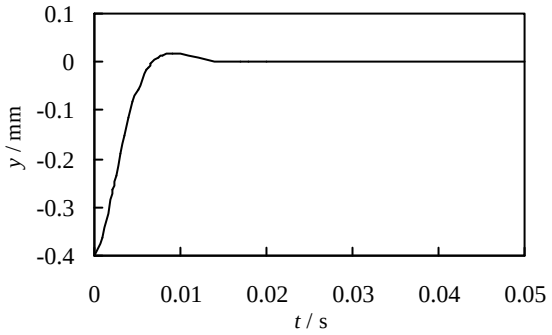

FIGURE 6: Step Response of Displacement

As the rotation axis is not equal to the rotor's inertial; the disturbances can be created by the unbalance of the rotor. It is modeled as a radial acceleration in the x-y plane with

$$\begin{cases} f_x = me_0\omega_r^2 \sin(\omega_r t) \\ f_y = me_0\omega_r^2 \cos(\omega_r t) \end{cases} \qquad (15)$$

Fig.7 shows x-y-plot of the rotor motion, the rotor speed is 40,000 rpm.

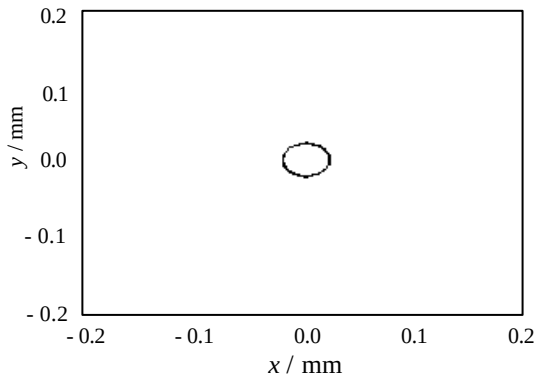

FIGURE 7: Orbit of Center

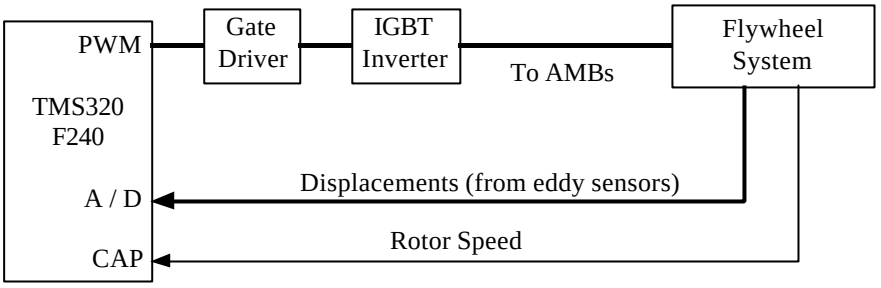

FIGURE 8: Experimental Configuration of DSP-based Control System

Experiment Result

A TMS320F240 fixed-point processor was used to execute the control algorithms. Fig.8 is the block diagram of experimental setup. Using the controller, the flywheel energy storage device has arrived at 40,000 rpm rotation speed, and it is able to provide about 0.5 kWh usable electrical energy. Fig.9 shows startup of the motor.

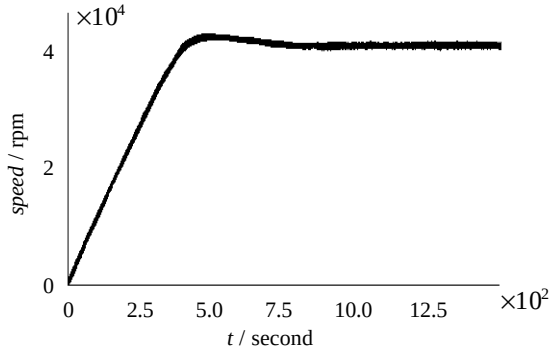

FIGURE 9: Startup of the Motor

CONCLUSIONS AND OUTLOOK

A flywheel energy storage device is studied, which has considered the influence of rotor's gyroscopic effects. A decoupling control approach is presented, which uses dynamic feedback linearization scheme. As a result, the potential rotor unstable brought by gyroscopic effects of the rotor can be avoided, the system achieve better performance.

A drawback of the decoupling control based on dynamic feedback linearization is that the controller is very sensitive to variation between the model and the real process. So a robust controller will be studied to overcome it. In addition, we are developing a kind of AMBs without bias current, which combine with permanent magnet bearing, so that energy consumption in system may be lower.

REFERENCES

1. A. Ahrens, A. Traxler, P. Von Burg, and G. Schweitzer. Design of a magnetically suspended flywheel energy storage device. Proc. 4th Int. Symp. on Magnetic Bearings, Zurich, Switzerland, 1994. 553-558
2. Yu Lie and Liu Heng. Bearing - Rotordynamics. Xi' an Jiaotong University Press, 1999 (in Chinese).
3. Schweitzer G, Traxler A, and Bleuler H. Magnetlager. Springer Verlag, 1993.
4. M. Ahrens, L. Kucera, and R. Larsonneur. Performance of a Magnetically Suspended Flywheel Energy Storage Device. IEEE Trans. CSC. Vol. 4, No.5, 1996, 494-502
5. A Chrara, J. De Miras, and B. Caron. Nonlinear Control of a Magnetic Levitation System without Premagnetization. IEEE Trans. CSC. Vol. 4, No.5, 1996. 513-523
6. Cao Jianrong, Yu Lie, and Xie Youbai. Decoupling Control for Active Magnetic Bearings. Journal of Xi' an Jiaotong University. Vol.33, No.12, 1999. 44-48 (in Chinese).
7. Cao Jianrong, Yu Lie, and Xie Youbai. Input-Output Linearizing Control for an Axial Magnetic Bearing. Journal of Xi' an Jiaotong University. Vol.34, No.10, 2000. 000-000 (in Chinese).
8. Cao Jianrong, Yu Lie, et al. Inverse System-Based Decoupling Control of Induction Motor. Trans. of China Electrotechnical Society. Vol. 14, No.1, 1999. 7-11 (in Chinese).